Perilipin 2 Improves Insulin Sensitivity in Skeletal Muscle Despite Elevated Intramuscular Lipid Levels

Madeleen Bosma,[1] Matthijs K.C. Hesselink,[2] Lauren M. Sparks,[1] Silvie Timmers,[1] Maria João Ferraz,[3] Frits Mattijssen,[4] Denis van Beurden,[1] Gert Schaart,[2] Marc H. de Baets,[5] Fons K. Verheyen,[6] Sander Kersten,[4] and Patrick Schrauwen[1]

Type 2 diabetes is characterized by excessive lipid storage in skeletal muscle. Excessive intramyocellular lipid (IMCL) storage exceeds intracellular needs and induces lipotoxic events, ultimately contributing to the development of insulin resistance. Lipid droplet (LD)–coating proteins may control proper lipid storage in skeletal muscle. Perilipin 2 (PLIN2/adipose differentiation–related protein [ADRP]) is one of the most abundantly expressed LD-coating proteins in skeletal muscle. Here we examined the role of PLIN2 in myocellular lipid handling and insulin sensitivity by investigating the effects of in vitro PLIN2 knockdown and in vitro and in vivo overexpression. PLIN2 knockdown decreased LD formation and triacylglycerol (TAG) storage, marginally increased fatty-acid (FA) oxidation, and increased incorporation of palmitate into diacylglycerols and phospholipids. PLIN2 overexpression in vitro increased intramyocellular TAG storage paralleled with improved insulin sensitivity. In vivo muscle-specific PLIN2 overexpression resulted in increased LD accumulation and blunted the high-fat diet–induced increase in protein content of the subunits of the oxidative phosphorylation (OXPHOS) chain. Diacylglycerol levels were unchanged, whereas ceramide levels were increased. Despite the increased IMCL accumulation, PLIN2 overexpression improved skeletal muscle insulin sensitivity. We conclude that PLIN2 is essential for lipid storage in skeletal muscle by enhancing the partitioning of excess FAs toward TAG storage in LDs, thereby blunting lipotoxicity-associated insulin resistance. *Diabetes* 61:2679–2690, 2012

Lipid droplets (LDs) serve an essential function in eukaryotic cells. Accordingly, intracellular lipid levels need to be tightly controlled. Indeed, inappropriate intracellular lipid storage leads to impaired cellular function. In obesity, lipids will overflow into the circulation as a result of lack of storage capacity in adipose tissue, and, as a consequence, lipids may accumulate ectopically in tissues, including skeletal muscle (intramyocellular lipids [IMCLs]). This ectopic fat storage exceeds intracellular demand and may result in lipotoxic events, including the development of insulin resistance (1,2). Paradoxically, IMCL is increased in both endurance-trained athletes and type 2 diabetic patients (3,4), indicating that ectopic lipid accumulation per se does not induce insulin resistance.

Thus far, explanations for this athlete's paradox have focused on lipid turnover, oxidative capacity, and levels of lipid intermediates (5–8). Interestingly, one exercise session was shown to prevent lipid-induced insulin resistance by partitioning more fatty acids (FAs) toward triacylglycerol (TAG) synthesis in skeletal muscle (9). Therefore, increasing the depot for TAG storage might improve insulin sensitivity. Intracellular TAG is stored in LDs, which are increasingly recognized as dynamic organelles. They are composed of a neutral lipid core containing TAG, diacylglycerol (DAG), cholesterolesters, retinol esters, and free cholesterol (10) surrounded by a phospholipid monolayer (11) and a protein coat, composed of a variety of LD-coating proteins (12). Accumulating evidence suggests that LD-coating proteins mediate LD dynamics, including LD synthesis, growth and fusion, intracellular transport, organelle interactions, and breakdown and lipolysis (13,14).

The best-characterized family of LD-coating proteins is the perilipin (PLIN) protein family, including PLIN1, PLIN2 (adipophilipin and adipose differentiation–related protein [ADRP]), PLIN3 (tail-interacting protein, 47 kDa [TIP47]), PLIN4 (adipocyte protein S3-12), and PLIN5 (OXPAT, lipid droplet storage protein 5 [LSDP5]). Whereas PLIN1 expression is restricted to adipose tissue, where it plays a crucial role in the control of storage and degradation of LDs (15,16), PLIN2 is expressed in several tissues, including liver, small intestine, and skeletal muscle (17,18). PLIN2 in skeletal muscle was previously shown to colocalize with IMCL (19). Interestingly, skeletal muscle *Plin2* gene expression was shown to be lower in patients with type 2 diabetes versus obese control subjects (20). Furthermore, weight loss as well as metformin treatment, both resulting in lower IMCL levels (21,22), were demonstrated to increase skeletal muscle PLIN2 levels in parallel with improved insulin sensitivity (23). PLIN2 may be involved in the protection against lipotoxicity by facilitating efficient IMCL storage in the form of TAG. However, loss- and gain-of-function studies to characterize PLIN2 function in skeletal muscle, required to obtain more functional insight into the role of PLIN2 in muscle, have not been performed to date. Here, we aimed to examine the role of PLIN2 in myocellular fat accumulation, lipotoxicity, and insulin sensitivity.

RESEARCH DESIGN AND METHODS

Cell culture experiments. C2C12 cells (LGC, Teddington, U.K.) were maintained in Dulbecco's modified Eagle's medium (DMEM) (Invitrogen,

Breda, the Netherlands) containing antibiotics supplemented with 10% FCS, grown on extracellular matrix (ECM) gel–coated (Sigma-Aldrich, St. Louis, MO) cell culture plates, and differentiated over the course of a week in DMEM supplemented with 2% FCS (differentiation media). Cells were treated with 200–800 μmol/L FAs (6–24 h) (octanoic, oleic, or palmitic acid conjugated to BSA; ratio BSA to FA, 1:2.5) or solely BSA as a control. For inhibitory RNA (RNAi) experiments, cells were transfected with 10 nmol/L Stealth RNAi oligos using Lipofectamine RNAiMAX (Invitrogen) as transfection reagent. PLIN2 overexpression was achieved by transfections with pENTR1A-pUC *Plin2* construct with Lipofectamine-2000 (Invitrogen).

Lipid metabolism. In vitro ^{14}C-palmitate metabolism was measured as previously described (24). Intracellular triglyceride levels were measured using the method of Schwartz and Wolins (25).

Glucose uptake assay. Glucose uptake was measured as previously described (26).

Animal studies. C57Bl6 mice were fed a low-fat (10% energy from fat) or a high-fat diet (HFD; 45% energy from fat) (Research Diet Services, Wijk bij Duurstede, the Netherlands) for 8 weeks. Tibialis anterior (TA) was dissected. Seven-week-old male Wistar rats were purchased from Charles River (Wilmington, MA). Rats were fed either a chow diet (*n* = 4) (SSNIFF; Bio Services, Uden, the Netherlands) or an HFD (*n* = 12) (45% energy from fat, D01060502; Research Diets, New Brunswick, NJ). The Institutional Animal Care and Use Committee of Maastricht University approved the experiments. The total intervention lasted 3 weeks. One week after the start of the diets, rats were cannulated, followed by gene electroporation and the hyperinsulinemic euglycemic clamp, with 1-week recovery periods in-between.

Electroporation. Overexpression of mouse PLIN2 in the left TA muscle of the rat was accomplished by an in vivo DNA electroporation technique under isoflurane anesthesia. Left TA muscles were transcutaneously injected with 75 μg pENTR1A-pUC *Plin2* construct, and right TA muscles were injected with empty vector as a control. Within 15 s after the last injection, one high-voltage pulse of 800 V/cm and four low-voltage pulses of 80 V/cm at 1 Hz were generated by an ECM 830 electroporator (BTX, San Diego, CA), as described previously (27).

Hyperinsulinemic euglycemic clamp. Clamps were performed as previously described (28). In brief, after a 6-h fast, a continuous infusion of insulin was administered at a rate of 13 mU/kg/min for 120 min. The glucose infusion rate was adjusted to maintain blood glucose concentration within the range of 4.5–5.5 mmol/L. Rats were conscious during the full procedure. At 45 min before completion of the clamp, a bolus of 140 μCi/kg of 2-(^{3}H(N))-deoxy-D-glucose was administered.

Lipid species. Skeletal muscle DAG, TAG, and ceramide levels were measured as previously described (28).

Western blots. Western blotting studies were performed using antibodies directed against PLIN2 (Progen, Heidelberg, Germany), PLIN3 (Santa Cruz, Heidelberg, Germany), PLIN5 (Progen), Akt phosphorylation (pAkt) and Akt, adipose triglyceride lipase (ATGL) (Cell Signaling Technology, Leiden, the Netherlands), comparative gene identification 58 (CGI-58) (Novus Biologicals, Littleton, CO), peroxisome proliferator–activated receptor γ coactivator 1-α (PGC1α) (Calbiochem, Amsterdam, the Netherlands), uncoupling protein 3 (UCP3) (provided by L.J. Slieker, Eli Lilly), and OXPHOS (Mitosciences, Eugene, OR). Protein expression values were standardized against actin protein expression (Sigma-Aldrich, St. Louis, MO). Secondary antibodies contained an infrared dye. Protein quantification was performed by scanning on an Odyssey Infrared Imaging System (LI-COR Biotechnology, Lincoln, NE).

Statistical analysis. Differences between groups were evaluated with univariate ANOVA followed by Tukey honestly significant difference post hoc tests (cell studies) and unpaired (cell studies) or paired Student *t* tests (animal experiments). *P* < 0.05 was considered statistically significant.

RESULTS

PLIN2 protein expression is induced upon lipid loading. We first examined if TAG accumulation in myotubes is indeed associated with altered expression of PLIN2. To this end, C2C12 mouse myotubes were incubated with different types of FAs (200 μmol/L) (Fig. 1*A*). Octanoate, a short-chain FA that is preferentially oxidized, did not increase TAG levels, whereas incubation with either oleate or palmitate led to marked accumulation of myocellular TAG as well as an increase in PLIN2 protein expression. The induction of PLIN2 protein levels was dependent on FA concentration, but reached the maximal induction at an FA concentration of 200 μmol/L (Supplementary Fig. 1*A*), and on FA incubation time, when the FA concentration was held constant at 200 μmol/L (Supplementary Fig. 1*B*). Next we

determined the in vivo effects of lipid overload on PLIN2 protein content. We found that both an 8-week HFD (Fig. 1*B*) and 6 or 24 h of fasting (Supplementary Fig. 1*C*) significantly increased PLIN2 protein levels in mouse skeletal muscle.

PLIN2 is essential for intracellular LD storage. To obtain further insight into the importance of PLIN2 for efficient TAG storage, we knocked down PLIN2 in myotubes using small interfering RNA (siRNA). Compared with PLIN2 levels in cells transfected with a scrambled control oligo, *Plin2* mRNA levels were reduced by 90% (Supplementary Fig. 2*A*) and protein levels decreased with 85% on average (Fig. 1*C*). The knockdown of PLIN2 prevented FA-induced TAG accumulation and LD formation even upon oleate or palmitate incubation, demonstrating that PLIN2 is essential for TAG storage in LDs (Fig. 1*D–F*). Protein expression of the LD-coating protein PLIN3 was not affected by PLIN2 knockdown, excluding a compensatory increase of this protein (Supplementary Fig. 2*B*). Please note that the LD-coating proteins PLIN1, PLIN4, and PLIN5 are not expressed in C2C12 cells. Electron microscopic imaging confirmed that oleate and palmitate led to massive lipid accumulation in control cells, whereas this lipid accumulation was largely absent after FA loading in the PLIN2 knockdown cells (Fig. 1*D* and *E*). The few LDs that were present in PLIN2 knockdown cells were markedly larger in size compared with control cells.

Knockdown of PLIN2 increases the cellular oxidative capacity. The lack of LD storage capacity in PLIN2 knockdown cells may be compensated by enhanced fat oxidative capacity or reduced FA uptake. To investigate these possibilities, we used an unbiased approach by implementing a whole-genome expression analysis in the PLIN2 knockdown cells (Fig. 2 and Table 1). Specifically, overrepresentation analysis of functional gene ontology classes showed suppression of numerous pathways related to FA transport and lipid storage (Fig. 2). Examples of genes that were downregulated upon PLIN2 knockdown include *Fads2* and *Agpat9* (Table 1). Furthermore, gene ontology classes corresponding to respiratory electron transport chain and glucose/carbohydrate metabolism were increased upon PLIN2 knockdown (Fig. 2), indicating a compensatory increase in expression of genes involved in mitochondrial function (average PLIN2 knockdown effect across treatment conditions: *Pgc1α* fold change (FC) = 3.2, *Mterf* FC = 2.2, *Mrps33* FC = 1.5, *Mfn1* FC = 1.3, and *Mtrf1l* FC = 1.8) (Table 1).

Consistent with the gene expression levels, knockdown of PLIN2 increased protein expression of OXPHOS complexes (total OXPHOS univariate ANOVA PLIN2 knockdown effect *P* < 0.05; complex I, *P* = 0.095; II, *P* = 0.052; III, *P* < 0.05; and V, *P* < 0.01) (Fig. 3*A* and Supplementary Fig. 3). Therefore, we next investigated whether PLIN2 knockdown resulted in a compensatory increased capacity to oxidize fat in order to deal with the lower capacity for lipid storage by measuring ^{14}C-palmitate oxidation. Knockdown of PLIN2 tended to increase total ^{14}C-palmitate oxidation (*P* = 0.055) (Fig. 3*B*). However, complete ^{14}C-palmitate oxidation to CO_2 was not affected (Fig. 3*C*). Instead, the tendency toward increased ^{14}C-palmitate oxidation can probably be ascribed to an increase in incomplete oxidation (acid-soluble metabolites [ASMs]; *P* = 0.108) (Fig. 3*D*). Thus, PLIN2 knockdown effects on palmitate oxidation were modest, indicating that the increased mitochondrial density only partly compensated for the reduction in TAG storage capacity.

Knockdown of PLIN2 increases palmitate incorporation into DAG and phospholipids. In the PLIN2 knockdown situation, the lack of the capacity to store FAs as TAG in LDs
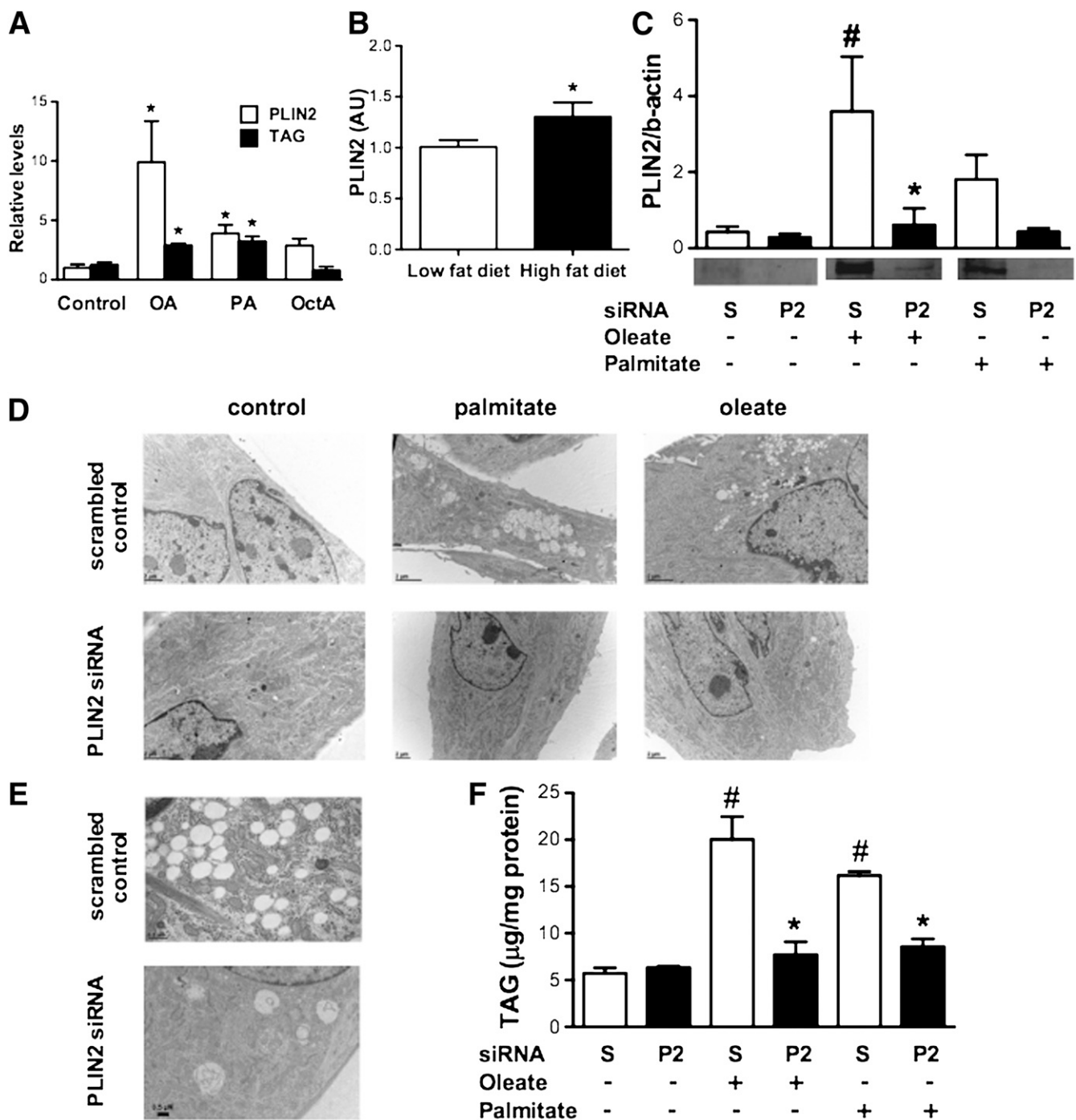
FIG. 1. PLIN2 knockdown lowers intracellular neutral lipid accumulation. *A*: C2C12 myotubes were incubated overnight with 80 μmol/L BSA complexed to 200 μmol/L oleate (OA), palmitate (PA), octanoate (OctA), or solely BSA as a control. PLIN2 and TAG levels are expressed as fold change relative to the control treatment. *P < 0.05 compared with the control treatment. *B*: PLIN2 protein expression in TA muscle of C57Bl6 mice fed an HFD or normal chow diet for 8 weeks. *C* and *D*: C2C12 myotubes were transfected with PLIN2 siRNA (P2) or a scrambled control (S) and incubated overnight with 200 μmol/L BSA-coupled oleate, palmitate, or solely 80 μmol/L BSA. Subsequently, cells were harvested to measure PLIN2 protein expression and TAG levels. #P < 0.05 vs. control (FA effect) and *P < 0.05 vs. scrambled control with the corresponding FA treatment. Data are expressed as mean ± SEM. *n* = 3–4. *D* and *E*: Electron microscopy pictures. *D* scale bars represent 2 microns. *E*: The oleate-treatment condition (increased LD size upon PLIN2 knockdown). Scale bars represent 0.5 micron.

resulted in a trend toward increased total FA oxidation, with the majority of ^{14}C-palmitate being incompletely oxidized and accounted for in ^{14}C-ASMs. Thus, another possibility to deal with FAs in the absence of cellular TAG storage capacity would be to store FAs in lipid species other than TAG. Therefore, ^{14}C-palmitate incorporation into total neutral lipids, TAG, DAG, and phospholipids was determined. Compared

with the scrambled control, a 3-h ^{14}C-palmitate incubation of PLIN2 knockdown cells resulted in a lower incorporation of palmitate in the total neutral lipid pool (*P* < 0.01) (Fig. 3*E*). Besides decreased total intracellular lipid storage, FA incorporation into neutral lipids shifted from TAG toward DAG and phospholipids. ^{14}C-palmitate incorporation into phospholipids and DAG was increased
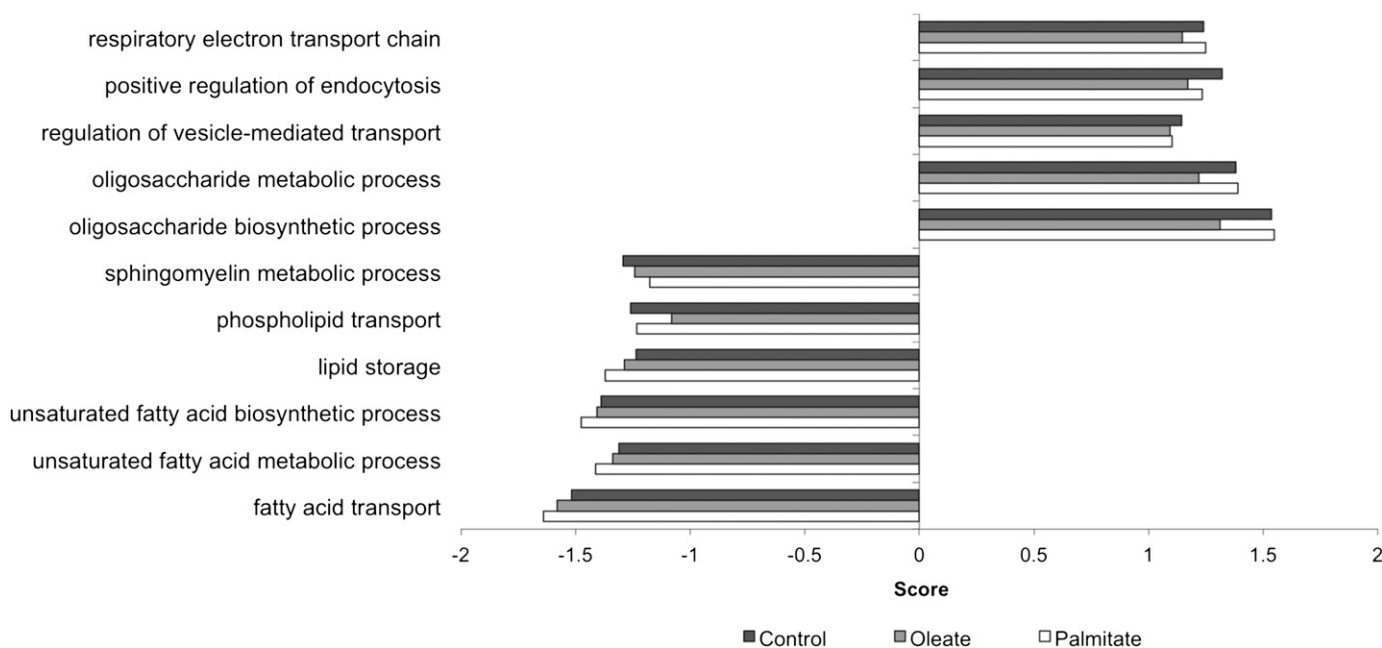
FIG. 2. Gene expression profiles of PLIN2 knockdown in C2C12 myotubes. Selected pathways identified by gene score resampling in ErmineJ. Only pathways that were significantly up- or downregulated ($P < 0.05$) are shown. The enrichment score reflects the degree to which a gene set is overrepresented at the top (upregulated, positive score) or bottom (downregulated, negative score) of the ranked gene list and is corrected for gene set size. Black bars, control condition; gray bars, oleate; white bars, palmitate treatment. Microarray data have been submitted to Gene Expression Omnibus (GSE38590).

in the PLIN2 knockdown cells compared with the scrambled control cells ($P < 0.01$ and $P < 0.05$, respectively), balancing the lower incorporation into TAG ($P < 0.01$) (Fig. 3F–H). PLIN2 knockdown did not compromise insulin signaling ($P = 0.0528$ for basal pAkt, $P = 0.82$ for insulin stimulated pAkt, and $P = 0.094$ for deoxyglucose uptake) (Fig. 3I and J).

In summary, PLIN2 is essential for LD formation and stability and intracellular TAG storage. PLIN2 knockdown increases FA oxidation only marginally.

PLIN2 overexpression protects against palmitate-induced impairments in insulin-stimulated glucose uptake. Lipid intermediate accumulation other than TAG storage is considered to negatively affect insulin signaling (30), whereas efficient TAG storage is considered harmless (28,31). Results from the PLIN2 knockdown studies illustrate that PLIN2 is necessary for efficient storage of FAs into inert TAG. Therefore, we next investigated whether overexpression of PLIN2 could facilitate efficient muscle TAG storage, and thereby prevent fat-induced impairments in insulin signaling. Hence, we overexpressed PLIN2 in vitro in order to investigate its potential beneficial effects on IMCL handling. PLIN2 overexpression resulted in a twofold increase in PLIN2 expression (Fig. 4A), a sixfold increased intracellular TAG storage ($P = 0.04$) (Fig. 4B), and increased ^{14}C-palmitate incorporation into total neutral lipids ($P = 0.013$), DAG, and TAG ($P = 0.003$ and $P = 0.042$, respectively) while decreasing its incorporation into phospholipids ($P = 0.006$) (Fig. 4C–F). We next tested if PLIN2-facilitated intramyocellular TAG storage could prevent palmitate-induced disruptions in insulin signaling. To this end, PLIN2- and empty vector–transfected C2C12 myotubes were incubated overnight with 400 μmol/L palmitate, known to impair insulin signaling (32). In line with the hypothesis, PLIN2 overexpression rescued palmitate-mediated impairments in insulin-stimulated glucose uptake ($P < 0.05$) (Fig. 4G).

In vivo, unilateral overexpression of PLIN2. To investigate if PLIN2 overexpression also has beneficial effects on insulin sensitivity in vivo, we overexpressed PLIN2 unilaterally in muscle of rats fed chow or HFD. We used an in vivo gene electroporation method to achieve ectopic PLIN2 expression in rat TA muscle in one leg, using the contralateral leg of the same animal as control. Marked overexpression of PLIN2 in rat TA muscle was obtained, as demonstrated by Western blotting (2.5-fold on average in whole-muscle lysates) (Fig. 5A), as well as immunofluorescence showing numerous LDs coated by PLIN2 (Fig. 5B). LDs in PLIN2-overexpressing muscle were larger and more numerous (Fig. 5B and C), indicating increased IMCL levels upon PLIN2 overexpression.

An unbiased whole-genome expression analysis revealed that genes related to lipid metabolism and mitochondrial FA oxidation were differentially regulated in PLIN2-electroporated versus control muscle in rats on the HFD (Table 2 and Supplementary Fig. 4). More specifically, examples of genes that were downregulated upon PLIN2 overexpression included *Pgc1α* (FC = −1.92), *Cpt2* (FC = −1.74), and the mitofusins (*Mfn1* FC = −1.53; *Mfn2* FC = −1.53) (Table 2). This group of downregulated genes was overrepresented in gene sets linked with oxidative phosphorylation, FA oxidation, and mitochondrial function (Supplementary Fig. 4) and included peroxisome proliferator–activated receptor α (PPARα) target genes (Supplementary Fig. 5). Upregulated genes included *SCD1* (FC = 1.62) and *PPARγ* (FC = 1.57) and were associated with gene sets related to lipid storage and carbohydrate metabolism (Table 2). Thus, PLIN2 overexpression was associated with a metabolic profile consistent with a shift from FA oxidation toward lipid storage.

TABLE 1
Expression patterns of a selection of genes in the six treatment conditions, derived from pools of four samples per treatment condition

Gene	GeneID	Gene name	Negative control			PLIN2 knockdown		
			Control	Oleate	Palmitate	Control	Oleate	Palmitate
Adfp	11520	Adipose differentiation–related protein	1	1.68	1.79	0.21	0.32	0.30
M6prbp1	66905	Mannose-6-phosphate receptor binding protein 1 (TIP47)	1	1.06	0.97	1.07	0.98	1.07
Dgke	56077	Diacylglycerol kinase, ε	1	1.23	0.66	1.81	2.02	1.97
Fads2	56473	Fatty acid desaturase 2	1	0.51	1.30	0.53	0.33	0.73
Pltp	18830	Phospholipid transfer protein	1	1.31	0.83	0.41	0.44	0.37
Smpdl3b	100340	Sphingomyelin phosphodiesterase, acid-like 3B	1	1.01	0.88	0.42	0.41	0.55
Elovl4	83603	Elongation of very long-chain fatty acids-like 4	1	0.99	0.85	0.65	0.70	0.53
Agpat4	68262	1-Acylglycerol-3-phosphate O-acyltransferase 4	1	1.01	0.91	0.51	0.57	0.57
Agpat9	231510	1-Acylglycerol-3-phosphate O-acyltransferase 9	1	1.33	1.42	0.50	0.61	0.59
Dgat2	67800	Diacylglycerol O-acyltransferase 2	1	0.84	0.75	0.60	0.53	0.58
Dhrs3	20148	Dehydrogenase/reductase (SDR family) member 3	1	1.30	1.95	0.58	0.74	0.66
Erlin2	244373	Endoplasmic reticulum lipid raft–associated 2	1	1.12	1.07	1.70	1.53	1.70
Erlin1	226144	Endoplasmic reticulum lipid raft–associated 1	1	1.25	1.13	1.47	1.68	1.70
Ppara	19013	PPARα	1	1.28	1.00	1.75	1.59	1.50
Ppargc1a	19017	PGC1α	1	1.12	0.81	3.46	2.96	2.95
Mterf	545725	Mitochondrial transcription termination factor	1	2.17	1.09	4.02	1.85	2.02
Mrps33	14548	Mitochondrial ribosomal protein S33	1	1.33	1.38	2.00	2.18	1.30
Car3	12350	Carbonic anhydrase 3	1	1.25	0.82	12.38	12.68	11.46
Mfn1	67414	Mitofusin 1	1	1.01	0.95	1.29	1.37	1.31
Cpt1b	12895	Carnitine palmitoyltransferase 1b, muscle	1	2.36	1.40	0.69	1.19	0.89
Mtrf1 L	108853	Mitochondrial translational release factor 1-like	1	1.40	1.26	2.32	2.07	1.93
Atp5g1	11951	ATP synthase, H+ transporting, mitochondrial F0 complex, subunit c isoform 1	1	1.92	0.91	1.04	2.73	0.97
Pdk2	18604	Pyruvate dehydrogenase kinase, isoenzyme 2	1	0.98	0.84	1.74	1.94	1.68
Mlycd	56690	Malonyl-CoA decarboxylase	1	1.82	1.01	1.19	1.67	1.57
Atp13a5	268878	ATPase type 13A5	1	1.05	0.72	2.85	2.68	2.31
Gk5	235533	Glycerol kinase 5	1	1.00	0.79	1.35	1.55	1.60
Lctl	235435	Lactase-like	1	0.64	0.95	0.31	0.25	0.29
Rrad	56437	Ras-related associated with diabetes	1	0.76	1.30	0.29	0.26	0.45
Rassf2	215653	Ras association (RalGDS/AF-6) domain familymember 2	1	1.09	0.78	0.23	0.20	0.27
Fgf21	56636	Fibroblast growth factor 21	1	0.77	0.84	0.21	0.23	0.20
Pld1	18805	Phospholipase D1	1	1.18	0.83	1.62	1.56	1.63
Atf3	11910	Activating transcription factor 3	1	1.05	1.97	0.40	0.43	0.42
Igfbp3	16009	Insulin-like growth factor binding protein 3	1	0.70	0.78	4.71	4.22	4.00
Mapk1	26413	Mitogen-activated protein kinase 1	1	1.08	0.92	1.31	1.28	1.35
Gga2	74105	Golgi-associated, γ adaptin ear containing, ARF binding protein 2	1	0.92	0.82	1.81	1.89	1.95
Gpr56	14766	G protein-coupled receptor 56	1	0.59	0.88	0.09	0.08	0.09
Purb	19291	Purine-rich element-binding protein B	1	1.01	1.16	0.46	0.47	0.51
Tnfrsf12a	27279	Tumor necrosis factor receptor superfamily, member 12a	1	0.84	1.11	0.59	0.64	0.55

Expression levels in scrambled control cells without FA treatment were set at 1, and expression levels in other groups were related to this reference condition. Microarray data have been submitted to Gene Expression Omnibus (GSE38590). Quantitative PCR was performed for a selection of genes to validate the microarray data (Supplementary Fig. 3).

PLIN2 overexpression induces changes in the expression of proteins involved in lipid metabolism. Western blottings were performed to extend the PLIN2 overexpression–mediated changes in gene expression to proteins involved in mitochondrial function (OXPHOS, PGC1α, and UCP3) and lipolysis (ATGL, CGI-58, and PLIN5). In the chow-fed group of animals, no significant changes in protein expression were observed upon PLIN2 overexpression. However, in rats fed the HFD for 4 weeks, protein levels of OXPHOS complexes I, III, and V tended to be decreased by PLIN2 overexpression ($P = 0.075$ for complex II) (Supplementary Fig. 6A), suggesting that the HFD-induced upregulation of OXPHOS protein expression was blunted by PLIN2 overexpression. These results corresponded with the observed lower gene expression levels of genes related to mitochondrial function and FA oxidation (Table 2 and Supplementary Fig. 4). PGC1α protein expression as well as PLIN5, another LD-coating protein that is supposed to be involved in oxidative processes (33), tended to be decreased upon PLIN2 overexpression
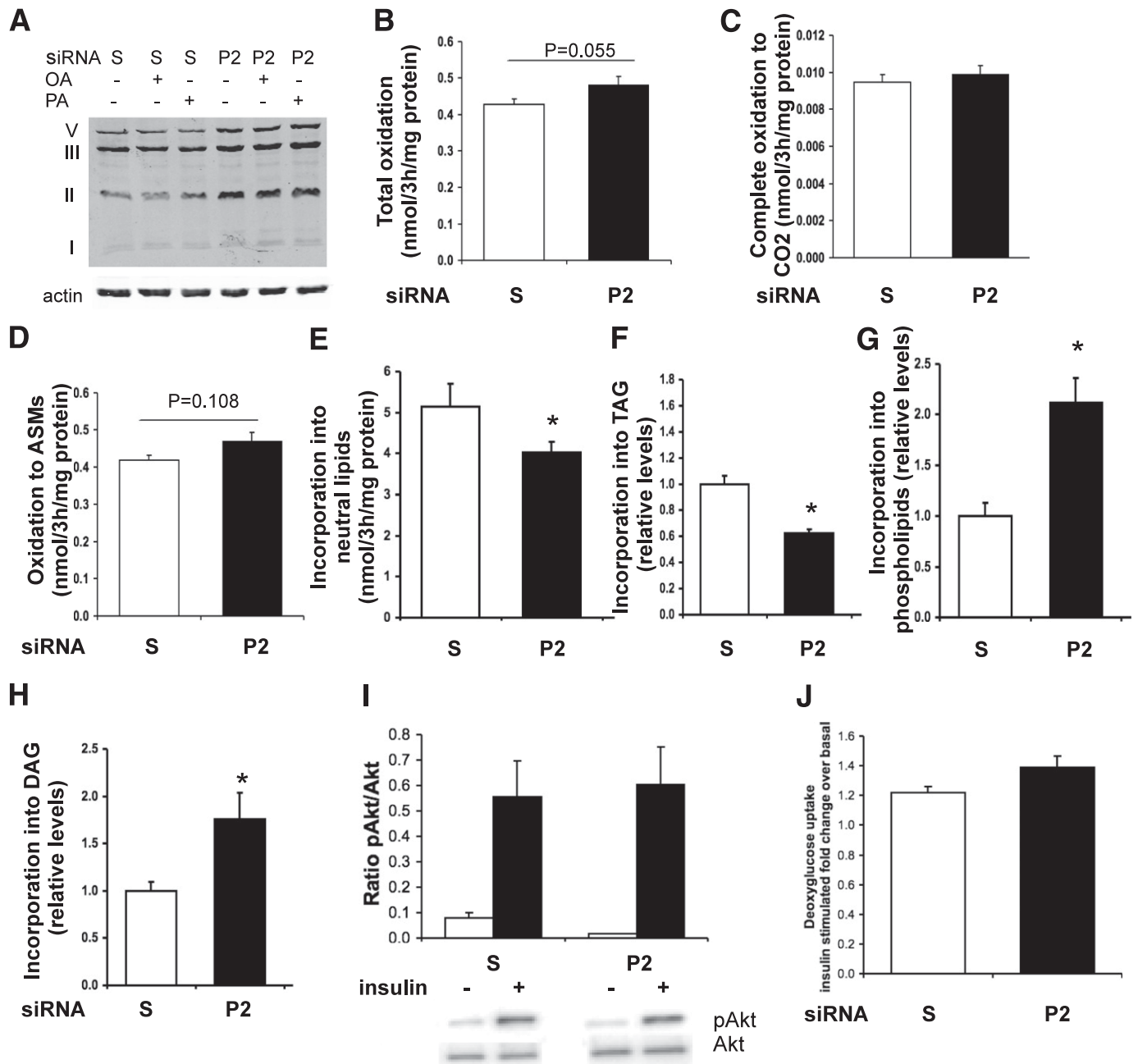
FIG. 3. Altered lipid metabolism and oxidative capacity in PLIN2 knockdown cells. *A*: Protein expression of the OXPHOS complexes I, II, III, and V in cell cultures transfected with either PLIN2 siRNA (P2) or scrambled control siRNA (S), expressed as arbitrary units (AU). *n* = 4 for each treatment condition. OA, oleate; PA, palmitate. Analysis of 3-h ^{14}C-FA oxidation rates in PLIN2 knockdown and negative control cells: total oxidation (sum of ^{14}C-CO$_2$ and ^{14}C ASMs) (*B*), complete oxidation to CO$_2$ (*C*), and incomplete oxidation to ASMs (*D*). *n* = 6 per treatment condition. ^{14}C-palmitate incorporation into total neutral lipids (*E*), TAG (*F*), phospholipids (*G*), and DAG (*H*). Values were normalized to protein levels. Incorporation into TAG, DAG, and phospholipids is expressed relative to the control condition. *I*: Insulin-stimulated deoxyglucose uptake. *J*: Insulin-stimulated pAkt phosphorylation. *P < 0.05. Error bars represent SEM.

(P = 0.062 and P = 0.078, respectively) (Supplementary Fig. 6*B* and *C*). Protein expression of ATGL, CGI-58, and UCP3 was not significantly changed (Supplementary Fig. 6*D–F*).

PLIN2 overexpression augments myocellular fat storage while blunting HFD-induced insulin resistance. We next investigated if the enhanced TAG storage capacity was associated with a reduction in the lipotoxic FA intermediates DAG and ceramides. Interestingly, despite increased IMCL accumulation, PLIN2 overexpression did

not increase DAG levels (Fig. 6*A*), nor was the FA composition (saturation and FA chain length) of the DAG fraction affected by PLIN2 overexpression (Supplementary Fig. 7). Thus, increased total IMCL levels in PLIN2-overexpressing muscle were not paralleled by increased DAG levels, indicating that FAs were stored as TAG. Intriguingly, ceramide levels were increased by 23% (Fig. 6*B*) upon PLIN2 overexpression.

PLIN2 overexpression thus increased IMCL levels concurrent with an altered gene expression profile favoring
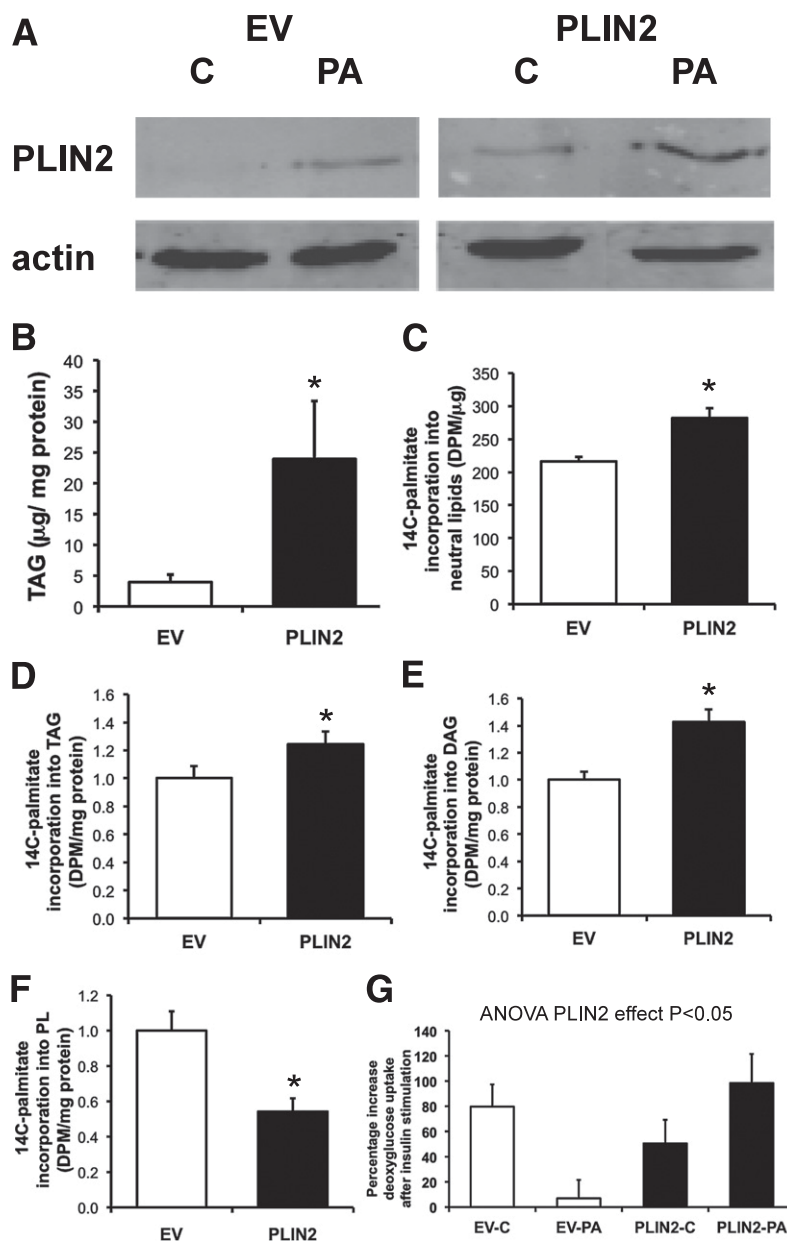
FIG. 4. PLIN2 overexpression protects against palmitate-induced insulin resistance in C2C12 myotubes. *A*: Western blot demonstrating efficiency of PLIN2 overexpression. *B*: TAG levels. Incorporation into neutral lipids (*C*), TAG (*D*), DAG (*E*), and phospholipids (PL) (*F*). Incorporation into TAG, DAG, and PL is expressed relative to the control condition. *G*: Insulin-stimulated deoxyglucose uptake. EV, empty vector; PA, palmitate (400 µmol/L); PL, phospholipids; C, control; DPM, disintegrations per minute. *$P < 0.05$. Error bars represent SEM.

efficient fat storage rather than oxidation. Therefore, we investigated whether these consequences of PLIN2 overexpression would affect insulin sensitivity. To this end, a hyperinsulinemic euglycemic clamp was implemented. As anticipated, rats on the HFD gained significantly more weight compared with the rats on a control (chow) diet (chow +1.91 ± 0.41 vs. HFD +2.94 ± 0.20 g/day, $P = 0.01$), and an HFD feeding period of 3 weeks sufficed to impede whole-body insulin sensitivity, as indicated by a lower glucose infusion rate during the stable phase of the clamp (chow 31.8 ± 1.0 vs. HFD 26.6 ± 1.6 mg/min/kg, $P = 0.05$). PLIN2 overexpression effects on insulin sensitivity were investigated in rats fed the HFD. During the stable phase of the clamp, ^{3}H-labeled deoxyglucose was administered intravenously to investigate muscle-specific deoxyglucose uptake, comparing the PLIN2-overexpressing TA muscle

with the control sham-electroporated muscle of the same rat. Interestingly, despite the profoundly increased total IMCL accumulation (Fig. 5*B* and *C*) and the increased ceramide levels (Fig. 6*B*), insulin sensitivity was not impaired in the PLIN2-overexpressing leg. Rather, deoxyglucose uptake significantly increased by 11.1% in the PLIN2-overexpressing leg compared with the control leg ($P = 0.045$) (Fig. 6*C*).

DISCUSSION

The protein coat of LDs is an important interface for the regulation of intracellular lipid metabolism. PLIN2 is one of the main LD-coating proteins in nonadipose tissues. In the current study, we demonstrate that PLIN2 plays an essential role in skeletal muscle IMCL storage. First, we
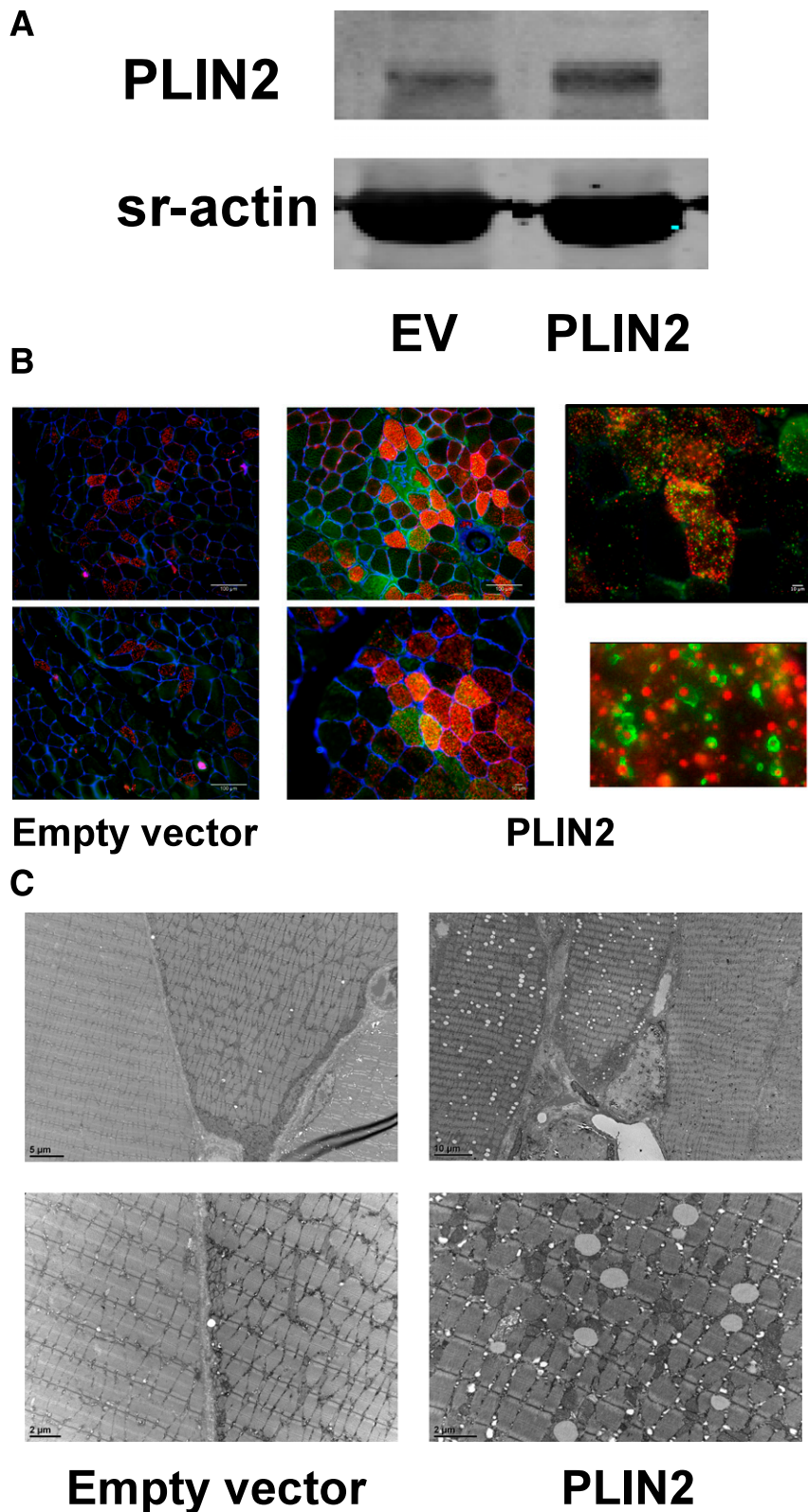
FIG. 5. Gene electrotransfer–mediated overexpression of PLIN2 in rat TA muscle. *A*: Representative Western blot demonstrating overexpression of PLIN2 in the left TA muscle. EV, empty vector. SR-actin, sarcomeric actin *B*: Lipid accumulation (red, Oil-Red-O) and PLIN2 expression (green) (overlap of PLIN2 and lipids appears yellow, but depends on the place of the cross-cut through the intracellular LDs) in TA muscle sections of the right (control, empty vector) and left (PLIN2 vector) leg of rats fed an HFD. Cell membranes are stained in blue. Representative pictures are shown. The image on the right bottom panel is a magnification of a selection of the picture above. *C*: Ultrastructure (transmission electron microscopy [TEM]) of muscle samples from sham- and PLIN2-electroporated muscle. (A high-quality digital representation of this figure is available in the online issue.)

TABLE 2
Heat map

ID	Fold change	Gene	Unigene	Description
308100	2.63	*Acat3*	Rn.203063	Acetyl-CoA acetyltransferase 3
100359680	2.43	*LOC100359680*	Rn.81758	Lysophosphatidylcholine acyltransferase 2-like
313220	2.39	*Acnat2*	Rn.162815	Acyl-CoA amino acid *N*-acyltransferase 2
29347	2.23	*Faah*	Rn.89119	Fatty acid amide hydrolase
499210	2.18	*Acer3*	Rn.19122	Alkaline ceramidase 3
500973	2.12	*Slc37a2*	Rn.224149	Solute carrier family 37 (glycerol-3-phosphate transporter), member 2
64035	2.09	*Pygl*	Rn.21399	Phosphorylase, glycogen
360622	2.05	*Igfbp4*	Rn.160666	Insulin-like growth factor binding protein 4
361401	1.99	*Pla2g15*	Rn.93631	Phospholipase A2, group XV
83730	1.94	*Vamp8*	Rn.82672	Vesicle-associated membrane protein 8
296474	1.93	*Pric285*	Rn.47450	PPAR A interacting complex 285
24377	1.91	*G6pd*	Rn.11040	Glucose-6-phosphate dehydrogenase
29411	1.9	*Ppt1*	Rn.1574	Palmitoyl-protein thioesterase 1
361527	1.9	*Pld3*	Rn.128036	Phospholipase D family, member 3
286896	1.83	*Sgpl1*	Rn.26953	Sphingosine-1-phosphate lyase 1
298199	1.76	*Adfp*	Rn.101967	Adipose differentiation-related protein
296371	1.7	*Pltp*	Rn.117434	Phospholipid transfer protein
288707	1.7	*Gltp*	Rn.4111	Glycolipid transfer protein
29560	1.7	*Hif1a*	Rn.10852	Hypoxia-inducible factor 1, α subunit (basic helix-loop-helix transcription factor)
314649	1.69	*S1pr4*	Rn.225785	Sphingosine-1-phosphate receptor 4
294422	1.68	*Smpdl3a*	Rn.8142	Sphingomyelin phosphodiesterase, acid-like 3A
361076	1.65	*RGD1561955*	Rn.200706	Similar to diacylglycerol kinase η
246074	1.64	*Scd1*	Rn.1023	Stearoyl-CoA desaturase 1
25096	1.63	*Pld1*	Rn.11130	Phospholipase D1
314360	1.6	*Galc*	Rn.30608	Galactosylceramidase
54315	1.59	*Ucp2*	Rn.13333	Uncoupling protein 2 (mitochondrial, proton carrier)
24334	1.58	*Eno2*	Rn.10828	Enolase 2, γ, neuronal
25664	1.57	*Pparg*	Rn.23443	PPAR γ
24654	1.53	*Plcb1*	Rn.45523	Phospholipase C, β 1 (phosphoinositide-specific)
25595	1.5	*Map2*	Rn.10484	Microtubule-associated protein 2
301265	−3.19	*Adhfe1*	Rn.90768	Phospholipase A2, group VII (platelet-activating factor acetylhydrolase, plasma)
291437	−2.61	*St3gal6*	Rn.199051	Lipase, endothelial
81782	−2.42	*Cxcl14*	Rn.59	Sterol *O*-acyltransferase 1
308100	−2.38	*Serhl2*	Rn.203063	Acetyl-CoA acetyltransferase 3
117243	−3.31	*Acsl6*	Rn.33697	Acyl-CoA synthetase long-chain family member 6
114508	−3.17	*Fbp2*	Rn.15319	Fructose-1,6-bisphosphatase 2
25747	−3.04	*Ppara*	Rn.9753	PPARα
291135	−2.71	*Acot13*	Rn.1730	Acyl-CoA thioesterase 13
79131	−2.28	*Fabp3*	Rn.32566	Fatty acid binding protein 3, muscle and heart
311617	−2.26	*Fitm2*	Rn.107822	Fat storage–inducing transmembrane protein 2
361637	−2.24	*Acsm5*	Rn.35367	Acyl-CoA synthetase medium-chain family member 5
117035	−2.05	*Slc25a20*	Rn.3289	Solute carrier family 25 (carnitine/acylcarnitine translocase), member 20
252898	−1.95	*Acox2*	Rn.10622	Acyl-CoA oxidase 2, branched chain
171142	−1.93	*Ehhadh*	Rn.3671	Enoyl-CoA, hydratase/3-hydroxyacyl CoA dehydrogenase
83516	−1.92	*Ppargc1a*	Rn.19172	PGC1α
64304	−1.87	*Acads*	Rn.1167	Acyl-CoA dehydrogenase, C-2 to C-3 short chain
29470	−1.84	*Mecr*	Rn.15375	Mitochondrial *trans*-2-enoyl-CoA reductase
25413	−1.74	*Cpt2*	Rn.11389	Carnitine palmitoyltransferase 2
305166	−1.72	*Agpat9*	Rn.214521	1-Acylglycerol-3-phosphate *O*-acyltransferase 9
25062	−1.7	*Gpd2*	Rn.89705	Glycerol-3-phosphate dehydrogenase 2, mitochondrial
305606	−1.69	*Mtif2*	Rn.160632	Mitochondrial translational initiation factor 2
25288	−1.68	*Acsl1*	Rn.6215	Acyl-CoA synthetase long-chain family member 1
25624	−1.68	*Vamp1*	Rn.31977	Vesicle-associated membrane protein 1
252900	−1.66	*Dgat2*	Rn.9523	Diacylglycerol *O*-acyltransferase homolog 2 (mouse)

TABLE 2
Continued

ID	Fold change	Gene	Unigene	Description
171155	−1.66	Hadhb	Rn.11253	Hydroxyacyl-CoA dehydrogenase/3-ketoacyl-CoA thiolase/enoyl-CoA hydratase (trifunctional protein), β subunit
29653	−1.65	Gpam	Rn.44456	Glycerol-3-phosphate acyltransferase, mitochondrial
25708	−1.57	Ucp3	Rn.9902	Uncoupling protein 3 (mitochondrial, proton carrier)
64476	−1.56	Mfn2	Rn.8570	Mitofusin 2
192647	−1.53	Mfn1	Rn.160939	Mitofusin 1
313510	−1.52	Atpaf1	Rn.18579	ATP synthase mitochondrial F1 complex assembly factor 1
353229	−1.52	Sgms1	Rn.55975	Sphingomyelin synthase 1
291567	−1.52	Ppargc1b	Rn.163382	PGC1β

Fold changes in gene expression for a selection of genes are given for PLIN2- versus empty vector–electroporated muscles. Quantitative PCR was performed for a selection of genes to validate the microarray data (Supplementary Fig. 4).

showed that PLIN2 is upregulated upon loading myotubes with long-chain FAs and after prolonged consumption of an HFD or fasting in skeletal muscle of mice. These findings served as a first indication for a role for PLIN2 in skeletal muscle lipid metabolism. In subsequent loss-of-function experiments, we demonstrate that PLIN2 plays an essential role in skeletal muscle lipid handling. siRNA-mediated knockdown of PLIN2 prevented intramyocellular TAG storage. Moreover, palmitate incorporation into DAG and phospholipids was increased, indicating that PLIN2 is necessary for FA channeling to TAG in LDs and that in the absence of PLIN2, part of the FAs are channeled to storage in the form of lipid intermediates other than TAG. Moreover, LD accumulation was restricted to a few LDs per myotube upon PLIN2 knockdown, indicating that PLIN2 is essential for the formation and/or stability of LDs. Studies toward subcellular localization of LDs indicated that PLIN2 might be involved in budding of LDs from endoplasmic reticulum (ER) or cell membrane structures (37,38). Functional involvement of PLIN2 in LD synthesis has been shown in studies in fibroblasts and liver (39–41). Our results support a role for PLIN2 in skeletal muscle LD synthesis, LD stability, and TAG storage.

Next to a lowering in intramyocellular TAG content after PLIN2 knockdown, we observed less LDs, but the few existing LDs per cell had a larger size, indicating that the cell copes with the flux of FAs entering the cells by maximizing the volume-to-surface ratio in the few available LDs. The latter is consistent with the study of Bell et al.

(42) in which PLIN2 knockdown was shown to decrease LD number while increasing LD size.

Enhancing the partitioning of excess FAs toward TAG storage is considered to be beneficial in preventing insulin resistance by limiting the accumulation of lipotoxic lipid species like ceramides, DAG, and fatty acyl-CoA (28,31). As our knockdown studies demonstrated that PLIN2 is essential for intramyocellular TAG storage, we investigated whether PLIN2 overexpression would influence lipid metabolism and lipid-induced insulin resistance. Therefore, we determined the effects of in vitro PLIN2 overexpression in C2C12 myotubes and in vivo unilateral, muscle-specific ectopic PLIN2 expression in rat TA muscle. PLIN2 overexpression markedly augmented the accumulation of TAG in LDs, which were both greater in number and larger in size, consistent with previous studies (40). Short-term incorporation of palmitate into both TAG and DAG was increased upon PLIN2 overexpression in myotubes, indicating increased channeling of FAs toward storage. Increased total IMCL levels upon prolonged PLIN2 overexpression in TA muscle (7 days) were not paralleled by increased intramyocellular DAG levels, indicating that FAs were efficiently stored as neutral TAG. Moreover, the gene expression profiles show a shift toward increased gene expression of genes involved in lipid storage, further supporting the notion that PLIN2 facilitates intramyocellular TAG storage.

The increase in TAG accumulation was not paralleled with an increased oxidative capacity. In contrast, the HFD-induced increase in mitochondrial density was blunted upon PLIN2 overexpression, and genes involved in FA
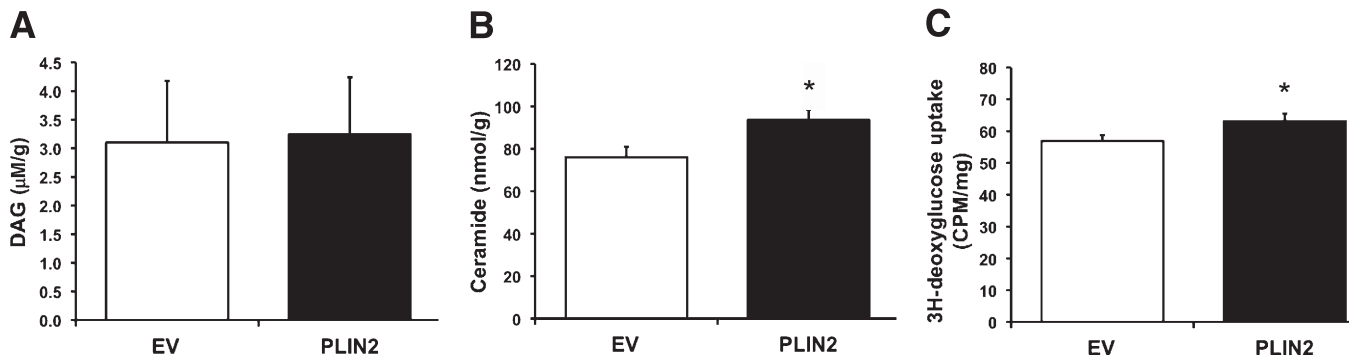

FIG. 6. Overexpression of PLIN2 in TA muscle of rats on an HFD improves insulin sensitivity of the muscle. Skeletal muscle DAG (*A*) and ceramide (*B*) levels in PLIN2- or empty vector (EV)–electroporated muscle of rats on an HFD. *C*: ^{3}H-labeled deoxyglucose uptake in control and PLIN2-electroporated TA muscle of rats on an HFD (*n* = 11). Error bars represent SEM. *$P < 0.05$.

oxidation and mitochondrial function were downregulated. One could hypothesize that an increased capacity to efficiently store TAG in muscle would diminish the need for an increased fat oxidative capacity. Decreased expression of genes and proteins involved in FA oxidation has been described previously in conditions of inhibited lipolysis (43,44). Recent studies show that the regulation of mitochondrial genes by their transcription factors PPARα and PGC1 requires FAs that are liberated by lipolysis from LD. Thus, ATGL-deficient mice are characterized by a marked reduction in mitochondrial function, which can be rescued by administration of the peroxisome proliferator–activated receptor agonist Wy14,643 (45). Likewise, PLIN2 overexpression decreased gene expression of several PPARα target genes. It could be hypothesized that PLIN2-facilitated LD storage reduces lipid turnover, leading to a reduced transcriptional activity of mitochondrial genes, consistent with the results of our microarray analysis. In that respect, studies in hepatocytes and embryonic kidney cells reported an increased lipolysis after PLIN2 knockdown (41,42,44), indicating that PLIN2 shields the droplet from lipolysis. A proper balance between IMCL synthesis, lipolysis, and oxidative metabolism ensures low local intracellular FA levels, thereby preventing lipotoxicity.

Our study is the first to examine the effects of overexpression of PLIN2 on insulin sensitivity. PLIN2 loss-of-function studies in tissues other than muscle showed inconsistent results on insulin sensitivity (42,46–48). Lowering of PLIN2 activity was demonstrated to improve liver insulin sensitivity in mouse models of PLIN2 inhibition (47,48), whereas siRNA-mediated knockdown of PLIN2 plus PLIN3 in liver cells impaired insulin sensitivity (42). In our study, we hypothesized that overexpression of PLIN2, by enhancing partitioning of excess fat toward TAG storage, would improve insulin sensitivity. Whereas, in vitro, PLIN2 knockdown in our hands did not affect insulin sensitivity, we did indeed find that PLIN2 overexpression completely rescued palmitate-induced impairments in insulin signaling, in parallel with increased intracellular TAG accumulation. We were able to extend this observation to the in vivo situation by showing improved insulin sensitivity in skeletal muscle of PLIN2-electroporated muscle of rats on an HFD, despite increased IMCL storage. Whereas IMCL levels were increased, DAG levels were unaffected and, unexpectedly, ceramide levels were increased upon PLIN2 overexpression. The latter is consistent with the study of Brown et al. (49), describing that increased ceramide levels associated with lowered lipase activity in liver did not impair insulin sensitivity (49). This leaves the option open that the subcellular localization of ceramide (rather than simply ceramide content) may be a determinant of the lipotoxic potential of ceramides.

One limitation of our in vivo study is that our results only apply to overexpression of PLIN2 in TA muscle, which is mainly composed of type IIb fibers. Yet, glycolytic muscles are prone to lipid-induced insulin resistance (50). Therefore, the observation that overexpression of PLIN2 resulted in excessive lipid storage in the predominantly glycolytic TA muscle while at the same time improving insulin-stimulated glucose uptake indicates that PLIN2-mediated improved partitioning of FAs in LDs is a potent way to blunt lipid-induced insulin resistance.

We conclude that high levels of PLIN2 are beneficial for proper storage of TAG in skeletal muscle and thereby prevent the development of insulin resistance. In that respect, we recently observed increased PLIN2 levels in skeletal muscle after training as well as in trained compared with untrained subjects (unpublished data), providing additional evidence that high PLIN2 levels, even with high IMCL content, are associated with improved insulin sensitivity. Likewise, Coen et al. (20) showed lower PLIN2 gene expression levels in skeletal muscle of insulin-resistant obese subjects versus BMI-matched insulin-sensitive controls, and both weight loss and pharmacological insulin-sensitizing strategies (troglitazone or metformin) resulted in increased PLIN2 protein levels in skeletal muscle (23).

In summary, using in vitro and in vivo methods, we establish that PLIN2 is an important facilitator of IMCL storage. PLIN2 is essential for myocellular TAG storage in LDs. By improving IMCL storage, PLIN2 protects from lipotoxicity, resulting in enhanced insulin sensitivity.

REFERENCES

1. Chow L, From A, Seaquist E. Skeletal muscle insulin resistance: the interplay of local lipid excess and mitochondrial dysfunction. Metabolism 2010;59:70–85
2. Goodpaster BH, Wolf D. Skeletal muscle lipid accumulation in obesity, insulin resistance, and type 2 diabetes. Pediatr Diabetes 2004;5:219–226
3. Goodpaster BH, He J, Watkins S, Kelley DE. Skeletal muscle lipid content and insulin resistance: evidence for a paradox in endurance-trained athletes. J Clin Endocrinol Metab 2001;86:5755–5761
4. van Loon LJC, Goodpaster BH. Increased intramuscular lipid storage in the insulin-resistant and endurance-trained state. Pflugers Arch 2006; 451:606–616
5. Bruce CR, Anderson MJ, Carey AL, et al. Muscle oxidative capacity is a better predictor of insulin sensitivity than lipid status. J Clin Endocrinol Metab 2003;88:5444–5451
6. Dubé JJ, Amati F, Stefanovic-Racic M, Toledo FGS, Sauers SE, Goodpaster BH. Exercise-induced alterations in intramyocellular lipids and insulin resistance: the athlete's paradox revisited. Am J Physiol Endocrinol Metab 2008;294:E882–E888
7. Meex RCR, Schrauwen-Hinderling VB, Moonen-Kornips E, et al. Restoration of muscle mitochondrial function and metabolic flexibility in type 2 diabetes by exercise training is paralleled by increased myocellular fat storage and improved insulin sensitivity. Diabetes 2010;59:572–579
8. Moro C, Bajpeyi S, Smith SR. Determinants of intramyocellular triglyceride turnover: implications for insulin sensitivity. Am J Physiol Endocrinol Metab 2008;294:E203–E213

9. Schenk S, Horowitz JF. Acute exercise increases triglyceride synthesis in skeletal muscle and prevents fatty acid-induced insulin resistance. J Clin Invest 2007;117:1690–1698

10. DiAugustine RP, Schaefer JM, Fouts JR. Hepatic lipid droplets. Isolation, morphology and composition. Biochem J 1973;132:323–327

11. Tauchi-Sato K, Ozeki S, Houjou T, Taguchi R, Fujimoto T. The surface of lipid droplets is a phospholipid monolayer with a unique fatty acid composition. J Biol Chem 2002;277:44507–44512

12. Wolins NE, Brasaemle DL, Bickel PE. A proposed model of fat packaging by exchangeable lipid droplet proteins. FEBS Lett 2006;580:5484–5491

13. Beller M, Thiel K, Thul PJ, Jäckle H. Lipid droplets: a dynamic organelle moves into focus. FEBS Lett 2010;584:2176–2182

14. Walther TC, Farese RV Jr. The life of lipid droplets. Biochim Biophys Acta 2009;1791:459–466

15. Blanchette-Mackie EJ, Dwyer NK, Barber T, et al. Perilipin is located on the surface layer of intracellular lipid droplets in adipocytes. J Lipid Res 1995;36:1211–1226

16. Greenberg AS, Egan JJ, Wek SA, Garty NB, Blanchette-Mackie EJ, Londos C. Perilipin, a major hormonally regulated adipocyte-specific phosphoprotein associated with the periphery of lipid storage droplets. J Biol Chem 1991;266:11341–11346

17. Heid HW, Moll R, Schwetlick I, Rackwitz H-R, Keenan TW. Adipophilin is a specific marker of lipid accumulation in diverse cell types and diseases. Cell Tissue Res 1998;294:309–321

18. Jiang HP, Serrero G. Isolation and characterization of a full-length cDNA coding for an adipose differentiation-related protein. Proc Natl Acad Sci USA 1992;89:7856–7860

19. Minnaard R, Schrauwen P, Schaart G, et al. Adipocyte differentiation-related protein and OXPAT in rat and human skeletal muscle: involvement in lipid accumulation and type 2 diabetes mellitus. J Clin Endocrinol Metab 2009;94:4077–4085

20. Coen PM, Dubé JJ, Amati F, et al. Insulin resistance is associated with higher intracellular triglycerides in type I but not type II myocytes concomitant with higher ceramide content. Diabetes 2010;59:80–88

21. Goodpaster BH, Theriault R, Watkins SC, Kelley DE. Intramuscular lipid content is increased in obesity and decreased by weight loss. Metabolism 2000;49:467–472

22. Teranishi T, Ohara T, Maeda K, et al. Effects of pioglitazone and metformin on intracellular lipid content in liver and skeletal muscle of individuals with type 2 diabetes mellitus. Metabolism 2007;56:1418–1424

23. Phillips SA, Choe CC, Ciaraldi TP, et al. Adipocyte differentiation-related protein in human skeletal muscle: relationship to insulin sensitivity. Obes Res 2005;13:1321–1329

24. Boschmann M, Engeli S, Moro C, et al. LMNA mutations, skeletal muscle lipid metabolism, and insulin resistance. J Clin Endocrinol Metab 2010;95:1634–1643

25. Schwartz DM, Wolins NE. A simple and rapid method to assay triacylglycerol in cells and tissues. J Lipid Res 2007;48:2514–2520

26. Hommelberg PP, Plat J, Sparks LM, et al. Palmitate-induced skeletal muscle insulin resistance does not require NF-κB activation. Cell Mol Life Sci 2011;68:1215–1225

27. Bruce CR, Hoy AJ, Turner N, et al. Overexpression of carnitine palmitoyltransferase-1 in skeletal muscle is sufficient to enhance fatty acid oxidation and improve high-fat diet-induced insulin resistance. Diabetes 2009;58:550–558

28. Timmers S, de Vogel-van den Bosch J, Hesselink MKC, et al. Paradoxical increase in TAG and DAG content parallel the insulin sensitizing effect of unilateral DGAT1 overexpression in rat skeletal muscle. PLoS ONE 2011;6:e14503

29. James DE, Jenkins AB, Kraegen EW. Heterogeneity of insulin action in individual muscles in vivo: euglycemic clamp studies in rats. Am J Physiol 1985;248:E567–E574

30. Samuel VT, Petersen KF, Shulman GI. Lipid-induced insulin resistance: unravelling the mechanism. Lancet 2010;375:2267–2277

31. Liu L, Shi X, Choi CS, et al. Paradoxical coupling of triglyceride synthesis and fatty acid oxidation in skeletal muscle overexpressing DGAT1. Diabetes 2009;58:2516–2524

32. Gaster M, Rustan AC, Beck-Nielsen H. Differential utilization of saturated palmitate and unsaturated oleate: evidence from cultured myotubes. Diabetes 2005;54:648–656

33. Wolins NE, Quaynor BK, Skinner JR, et al. OXPAT/PAT-1 is a PPAR-induced lipid droplet protein that promotes fatty acid utilization. Diabetes 2006;55:3418–3428

34. Fan B, Ikuyama S, Gu J-QIU, et al. Oleic acid-induced ADRP expression requires both AP-1 and PPAR response elements, and is reduced by pycnogenol through mRNA degradation in NMuLi liver cells. Am J Physiol Endocrinol Metab 2009;297:E112–E123

35. Gao J, Ye H, Serrero G. Stimulation of adipose differentiation related protein (ADRP) expression in adipocyte precursors by long-chain fatty acids. J Cell Physiol 2000;182:297–302

36. Grasselli E, Voci A, Pesce C, et al. PAT protein mRNA expression in primary rat hepatocytes: effects of exposure to fatty acids. Int J Mol Med 2010;25:505–512

37. Gao J, Serrero G. Adipose differentiation related protein (ADRP) expressed in transfected COS-7 cells selectively stimulates long chain fatty acid uptake. J Biol Chem 1999;274:16825–16830

38. Robenek H, Hofnagel O, Buers I, Robenek MJ, Troyer D, Severs NJ. Adipophilin-enriched domains in the ER membrane are sites of lipid droplet biogenesis. J Cell Sci 2006;119:4215–4224

39. Chang BH, Li L, Paul A, et al. Protection against fatty liver but normal adipogenesis in mice lacking adipose differentiation-related protein. Mol Cell Biol 2006;26:1063–1076

40. Imamura M, Inoguchi T, Ikuyama S, et al. ADRP stimulates lipid accumulation and lipid droplet formation in murine fibroblasts. Am J Physiol Endocrinol Metab 2002;283:E775–E783

41. Listenberger LL, Ostermeyer-Fay AG, Goldberg EB, Brown WJ, Brown DA. Adipocyte differentiation-related protein reduces the lipid droplet association of adipose triglyceride lipase and slows triacylglycerol turnover. J Lipid Res 2007;48:2751–2761

42. Bell M, Wang H, Chen H, et al. Consequences of lipid droplet coat protein downregulation in liver cells: abnormal lipid droplet metabolism and induction of insulin resistance. Diabetes 2008;57:2037–2045

43. Pinent M, Hackl H, Burkard TR, et al. Differential transcriptional modulation of biological processes in adipocyte triglyceride lipase and hormone-sensitive lipase-deficient mice. Genomics 2008;92:26–32

44. Sapiro JM, Mashek MT, Greenberg AS, Mashek DG. Hepatic triacylglycerol hydrolysis regulates peroxisome proliferator-activated receptor-alpha activity. J Lipid Res 2009;50:1621–1629

45. Wölkart G, Schrammel A, Dörffel K, Haemmerle G, Zechner R, Mayer B. Cardiac dysfunction in adipose triglyceride lipase deficiency: treatment with a PPARα agonist. Br J Pharmacol 2011;165:380–389

46. Chang BH-J, Li L, Saha P, Chan L. Absence of adipose differentiation related protein upregulates hepatic VLDL secretion, relieves hepatosteatosis, and improves whole body insulin resistance in leptin-deficient mice. J Lipid Res 2010;51:2132–2142

47. Imai Y, Varela GM, Jackson MB, Graham MJ, Crooke RM, Ahima RS. Reduction of hepatosteatosis and lipid levels by an adipose differentiation-related protein antisense oligonucleotide. Gastroenterology 2007;132:1947–1954

48. Varela GM, Antwi DA, Dhir R, et al. Inhibition of ADRP prevents diet-induced insulin resistance. Am J Physiol Gastrointest Liver Physiol 2008;295:G621–G628

49. Brown JM, Betters JL, Lord C, et al. CGI-58 knockdown in mice causes hepatic steatosis but prevents diet-induced obesity and glucose intolerance. J Lipid Res 2010;51:3306–3315

50. Levin MC, Monetti M, Watt MJ, et al. Increased lipid accumulation and insulin resistance in transgenic mice expressing DGAT2 in glycolytic (type II) muscle. Am J Physiol Endocrinol Metab 2007;293:E1772–E1781